Proceedings of the 12th International Conference on
Aluminium Alloys, September 5-9, 2010, Yokohama, Japan

pp. 902-907

Evolution of Grain Structure During Superplastic Deformation of an Al-Zn-Mg-Cu-Zr Alloy Containing Sc

Ashim Kumar Mukhopadhyay[1], Amit Kumar[1], Konduri Satya Prasad[1], Siriki Raveendra[2] and Indradev Samajdar[2]

[1]Defence Metallurgical Research Laboratory, Kanchanbagh, Hyderabad-500 058, India

[2]Indian Institute of Technology Bombay, Powai, Mumbai-400 076, India

Recent studies have shown that suitably thermo-mechanically processed (TMP) Al-Zn-Mg-Cu-Zr-Sc alloys having essentially an unrecrystallized grain structure may be subjected to superplastic deformation at 475°C, $1.9 \times 10^{-2}s^{-1}$ to obtain a total elongation of 650%. The present work demonstrates that the utilization of two-step strain rate at 425°C during superplastic deformation of the similarly thermo-mechanically processed alloy increases the total elongation value to as high as 916%. The beneficial effect of two-step strain rate could further be realized at 350°C to obtain a total elongation of 438%. Using a combination of transmission electron microscopy (TEM) and electron back scattered diffraction (EBSD), the present work provides a systematic assessment of the changes in percentage recrystallization and recrystallized grain size with percentage elongation in the material during superplastic deformation. The percentage recrystallization and the average size of the recrystallized grains increase gradually with the percentage elongation. The final grain structure has an average recrystallized grain size of less than 10 μm under all deformation conditions studied in this work. The stability of the fine recrystallized grains due to the presence of both Zr and Sc in the alloy is understood to be the key toward achieving enhanced superplasticity.

Keywords: *Al-Zn-Mg-Cu-Zr-Sc alloy; two-step strain rate; superplasticity; transmission electron microscopy; electron back scattered diffraction*

1. Introduction

Superplastic deformation studies using high strength 7xxx series Al alloys containing either Zr and/or a combination of both Zr and Sc have demonstrated that the presence of these dispersoid forming elements make static recrystallization difficult [1-3]. The influence of Zr and Sc additions on the inhibition of static recrystallization in 7xxx series alloys is, therefore, similar to those observed in other grades of Al alloys [4, 5]. However, dynamic recrystallization does occur in such alloys under suitable combinations of temperature and strain rate during superplastic deformation, thereby facilitating the attainment of high percentage of total elongation [1-4]. Studies using Al-Zn-Mg-Cu-Zr alloy 7449 further established that the utilization of two-step strain rate [6, 7] (in the sequence of a higher strain rate followed by a lower strain rate) at a suitable temperature improved the total percentage of elongation significantly [1, 2].

The purpose of the present investigation involving the Al alloy 7010 containing Sc is two fold. Firstly, it is to examine the influence of two-step strain rate at two different temperatures on the attainment of total percentage elongation during superplastic deformation. It is to be considered that the advantages associated with the utilization of two-step strain rate are (i) the increase in percentage elongation, as well as (ii) the reduction in the time required to deform the material. The latter has a significant commercial implication, because a major problem associated with the superplastic forming of aerospace materials has been the low forming rate i.e. $<10^{-2}s^{-1}$. The other purpose of this work is to ascertain how and at what stage recrystallization occurs in the material during the superplastic tensile deformation. Further to be ascertained is the percentage recrystallization in the alloy following the attainment of the maximum total percentage of elongation during the superplastic

deformation. This is because, the occurrence of recrystallization is known to be extremely difficult in Al alloys containing both Sc and Zr [1-5].

2. Experimental Procedure

The alloy used in the present investigation has the composition (wt%) of Al-6.3Zn-2.3Mg-1.5 Cu-0.14Zr-0.23Sc-0.04Fe-0.02Si. Fe and Si impurities were associated with the primary aluminium that was used to prepare the alloy. The alloy was prepared in an induction furnace under argon atmosphere, homogenized and scalped. The resultant slabs (395 mm × 300 mm × 85 mm) were then soaked at 435°C for 4 h followed by rolling to produce plates of thickness 15 mm. While rolling down the slabs from 85 to 15 mm thickness, intermediate annealing was given each time at 435°C for 25 min following 7% reduction in thickness. The resultant 15 mm thick plates were then subjected to a 3-step thermo-mechanical process in the following sequence: (1) solutionizing at 465°C for 1 h followed by quenching in water, (2) over aging at 400°C for 8 h, and (3) hot rolling at 400°C to produce 2.3 mm thick sheets (without any intermediate annealing).

Flat tensile samples were machined from 2.3 mm thick sheets to carry out incremental velocity tensile tests [6] at various temperatures and strain rates ranging from 425 to 475°C and 3×10^{-5} to $1.9 \times 10^{-2} s^{-1}$. Constant strain rate tensile tests were then performed at appropriate combination of temperatures and strain rates to determine the total elongation. For the present alloy, the highest 'm' value of 0.70 was obtained at 475°C, $1.9 \times 10^{-2} s^{-1}$, and the maximum elongation of 650% was obtained when deformed at this temperature, strain rate combination [1, 3]. While utilizing the beneficial effect of two-step strain rate on the percentage elongation, it is necessary to avoid the upper end of the temperature range, otherwise found to be suitable for superplastic deformation of the alloy using one-step strain rate. This is because, under a combination of both high temperature and the accelerated strain rate (i.e. the first step of the two-step strain rate), both nucleation as well as growth of the recrystallized grains would occur. The growth of the recrystallized grains is not a welcome feature at any stage of the superplastic deformation process. As a result, in the present study, the optimum temperature for superplastic deformation while using the two-step strain rate was found out to be 425°C. Furthermore, the two-step strain rate was applied in the sequence of a higher strain rate (up to the strain value of $\varepsilon = 0.73$, as determined by trials, at the strain rate value of $10^{-1} s^{-1}$) followed by a lower strain rate of $10^{-2} s^{-1}$.

In the present study, the superplastic deformation of the alloy was further carried out at 350°C both using one-step strain rate of $10^{-3} s^{-1}$, and two-step strain rates of $10^{-2} s^{-1}$ (up to the strain value of $\varepsilon = 0.5$) and $10^{-3} s^{-1}$. This was to examine the influence of the two-step strain rate on the percentage elongation of the alloy at lower temperatures.

A combination of TEM and EBSD was utilized to examine the grain structure developed in the TMP material and those developed during the superplastic deformation. Unless otherwise stated, the location of samples for the microstructural studies of the superplastically deformed materials was confined to the center of the gauge length. TEM was carried out on a FEI TECNAI 20T electron microscope operating at 200 kV. Selected area electron diffraction patterns (SAEDPs) obtained from different regions of the thin foils were utilized to distinguish between recrystallized and unrecrystallized portions of the material. In EBSD analysis, a combined criterion of grain size and in-grain misorientation was used [8, 9] to distinguish between deformed / unrecrystallized and recrystallized regions of the material. Grains with less than 2° grain orientation spread (GOS), above 2 μm in size and having continuous boundaries of 5° or more misorientation were considered to be recrystallized regions, while regions that did not meet either of these conditions were considered to be deformed. The EBSD measurements / scans were made using FEI Quanta 3D FEG instrument located at the National Facility on OIM and Texture (a DST-IRPHA facility), Department of Metallurgical Engineering and Materials Science, IIT Bombay.

3. Results and Discussion

Figure 1(a) represents a transmission electron micrograph obtained from the 2.3 mm thick TMP sheets, showing the presence of subgrains elongated along the rolling direction. TEM studies failed to locate any recrystallized grain in the microstructure. Figure 1(b) represents a typical EBSD image obtained from the TMP sheets, and Figure 1(c) represents the corresponding recrystallization data, as partitioned from (b). Analysis of the data obtained from Figure 1(c) showed the percentage recrystallization to be as low as 0.2% and an average recrystallized grain size of 2.4 μm. The grain structure developed in the TMP sheets could, therefore, be best described as "essentially unrecrystallized". Enlargement of a selected portion of the EBSD image presented in Figure 1(b) does show the presence of elongated subgrains [one marked by arrows in (d)] in the microstructure.

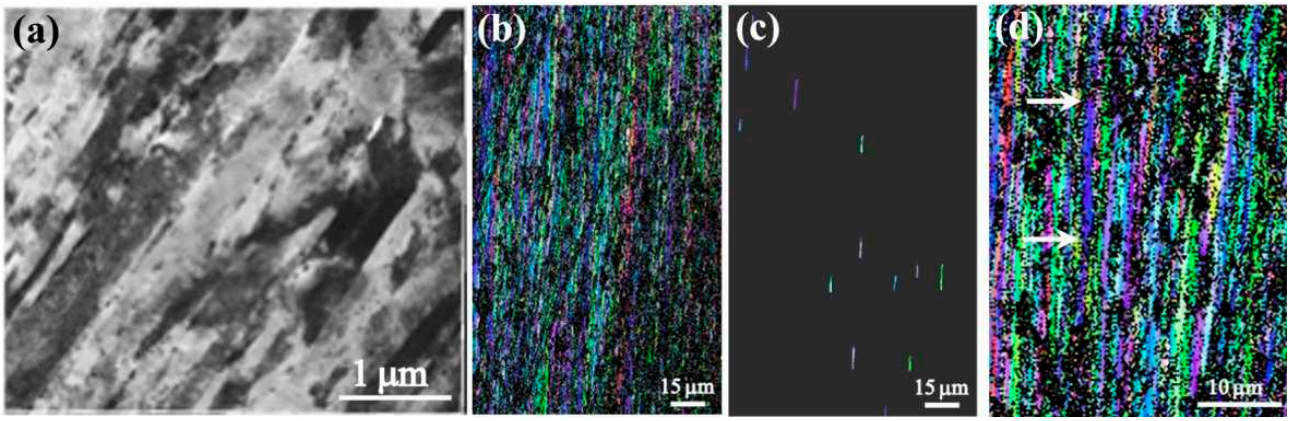

Fig. 1. (a) Transmission electron micrograph showing subgrains elongated along the rolling direction in the TMP sheets, (b) Typical EBSD image obtained from the TMP sheets, (c) Recrystallization data, as partititoned from (b), and (d) Portion of the image in (b), when enlarged, showing elongated subgrains (one marked by arrows).

Figures 2(a) through (f) represent transmission electron micrographs of the alloy tested at 475°C, $1.9 \times 10^{-2}s^{-1}$ after interrupting the tensile test at strain values of $\varepsilon = 0.34$ (40% elongation), (b) & (c) $\varepsilon = 0.69$ (100% elongation), (d) $\varepsilon = 1.10$ (200% elongation), (e) $\varepsilon = 1.39$ (300% elongation) and (f) $\varepsilon = 1.79$ (500% elongation), respectively. The most noticeable feature in Figure 2(a), when compared with Figure 1(a), is the growth of the subgrains under a combination of suitable strain rate and temperature. The rotation of subgrains is understood to be mainly responsible for the growth of the suitably oriented subgrains at the expense of the neighbouring subgrains (the arrows in (a) show the directions of local migration of subgrain boundaries). Such subgrains eventually merge with the transition bands, thereby converting subgrain boundaries into high angle boundaries.

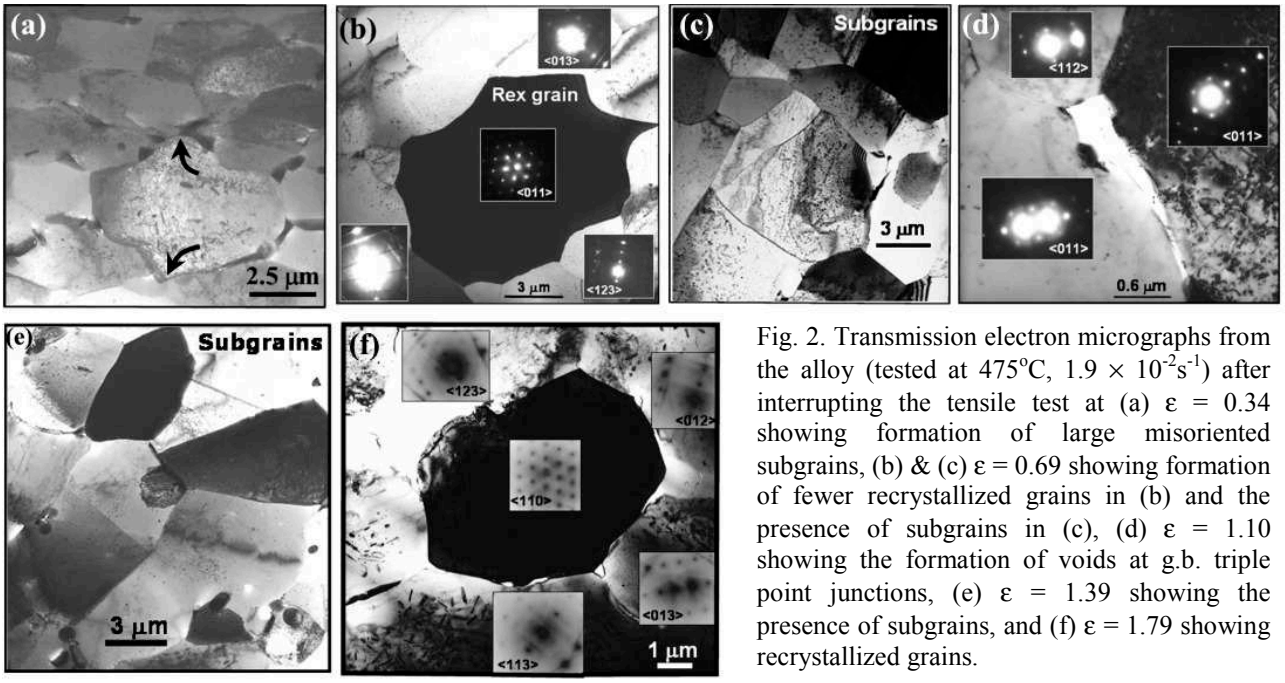

Fig. 2. Transmission electron micrographs from the alloy (tested at 475°C, $1.9 \times 10^{-2}s^{-1}$) after interrupting the tensile test at (a) $\varepsilon = 0.34$ showing formation of large misoriented subgrains, (b) & (c) $\varepsilon = 0.69$ showing formation of fewer recrystallized grains in (b) and the presence of subgrains in (c), (d) $\varepsilon = 1.10$ showing the formation of voids at g.b. triple point junctions, (e) $\varepsilon = 1.39$ showing the presence of subgrains, and (f) $\varepsilon = 1.79$ showing recrystallized grains.

Figure 2(b) shows the formation of fewer recrystallized grains, as evidenced by the SAEDPs (see insets) showing high angles of misorientation across the grain boundaries of the new grains. Figure 2(c) shows the presence of subgrains in a different region of the same thin foil. At this stage of the deformation, TEM did not detect any void in the material. The presence of voids, often located at grain boundary triple point junctions was detected after 200% elongation as shown in Figure 2(d). Further, although the number density of the recrystallized grains increased with percentage elongation, TEM could readily detect the presence of subgrains even after 300% elongation as shown in Figure 2(e). On the other hand, TEM could detect only recrystallized grains in the alloy sample after 500% elongation, as shown in Figure 2(f).

Figures 3(a) through (e) represent recrystallization data, as partitioned from the EBSD images of the alloy tested at 475°C, $1.9 \times 10^{-2}s^{-1}$ after interrupting the tensile test at various strain values. It may be noted that the percentage recrystallization (labeled on each micrograph) increased gradually with the percentage elongation. The average size of the recrystallized grain (labeled on each micrograph) also increased gradually with the percentage elongation. Beyond 200% elongation, both the percentage recrystallization as well as the formation of voids/cavitations increased significantly (as evidenced by TEM) and this behaviour is reflected by the appreciable drop in the σ value beyond the ε value of 1.10 in the stress (σ) vs. strain (ε) curve of the alloy tested at 475°C, $1.9 \times 10^{-2}s^{-1}$ [see Figure 3(f)].

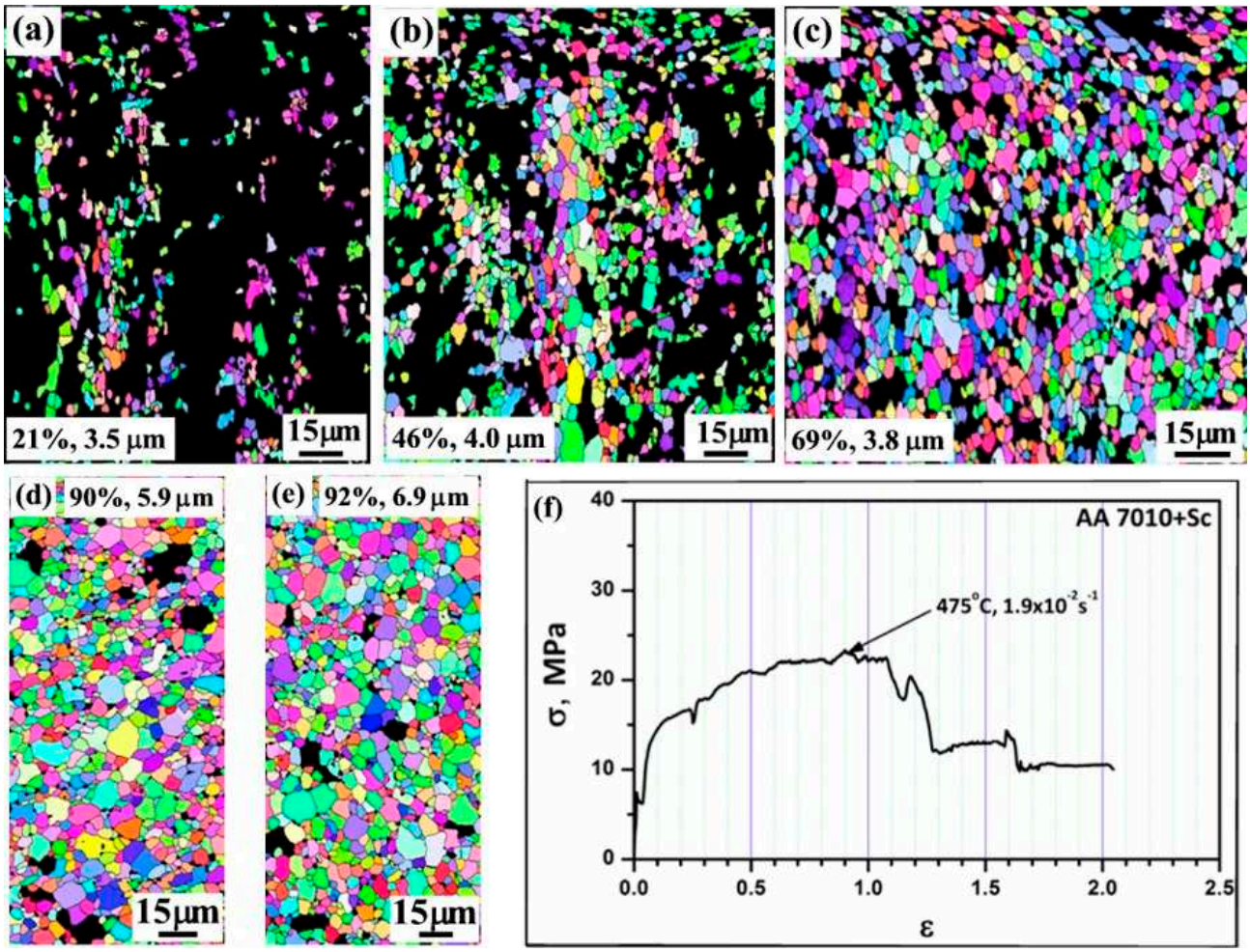

Fig.3. Recrystallization data, as partitioned from the EBSD images of the alloy tested at 475°C, $1.9 \times 10^{-2}s^{-1}$ after interrupting the tensile test at strain rate, elongation values of (a) 0.34, 40%, (b) 0.69, 100%, (c) 1.10, 200%, (d) 1.79, 500%, and (e) 2.01, 650%, respectively. Percentage recrystallization, recrystallized grain size values in each case are labeled on the micrographs. (f) Plot of stress (σ) vs. strain (ε) of the alloy tested at 475°C, $1.9 \times 10^{-2}s^{-1}$. The dark portions in the micrographs represent deformed regions.

Figures 4(a) through (c) show the photographs of the (a) original tensile sample, and the samples tested at (b) 425°C, $10^{-2}s^{-1}$ and (c) 425°C, $10^{-1}s^{-1} + 10^{-2}s^{-1}$, respectively. Figures 5(a) and (b) represent recrystallization data, as partitioned from the EBSD images of the alloy samples tested using (1) one-step and (2) two-step strain rate, respectively. In both cases, the percentage recrystallization recorded was 89%, although in the case of the two-step strain rate sample, the average recrystallized grain size was relatively finer. The use of two-step strain rate increased the total percentage elongation from 562 to 916%.

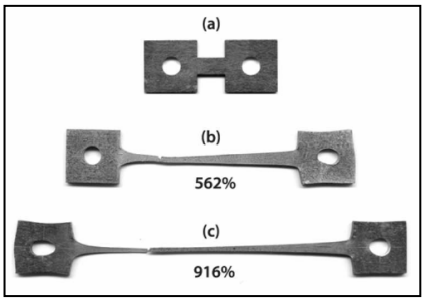

Fig. 4. Photographs of flat tensile samples of the alloy (a) original, (b) tested at 425°C, $10^{-2}s^{-1}$ and (c) tested at 425°C, $10^{-1}s^{-1}$ ($\varepsilon = 0.73$) + $10^{-2}s^{-1}$.

Figures 5(c) and (d) represent recrystallization data, as partitioned from the EBSD images of the alloy samples tested at 350°C, $10^{-3}s^{-1}$ and 350°C, $10^{-2}s^{-1} + 10^{-3}s^{-1}$, respectively. The percentage recrystallization greatly increased from 68% (with an average grain size of 3.5 μm) for the one-step strain rate sample to 81% (within an average grain size of 3.9 μm) for the two-step strain rate sample. Associated with this is the corresponding increase in the total percentage elongation from 360 to 438%.

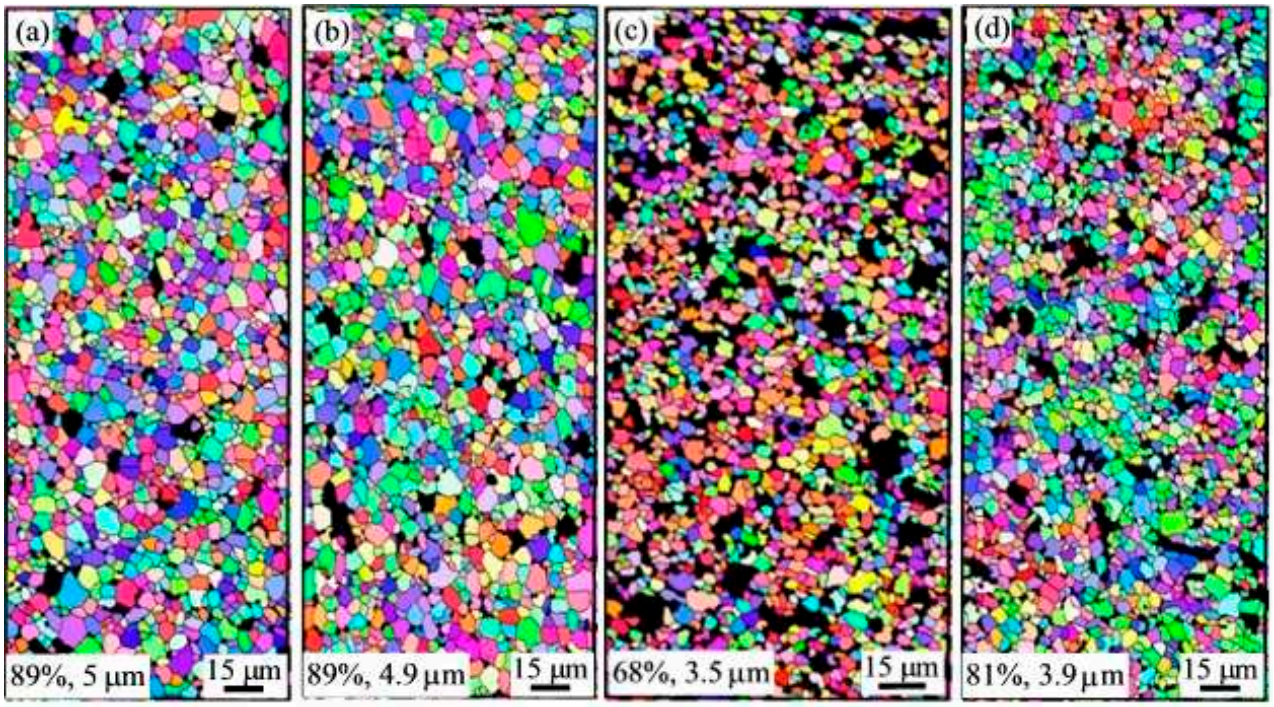

Fig. 5. Recrystallization data, as partitioned from the EBSD images from the alloy tested at (a) 425°C, $10^{-2}s^{-1}$, (b) 425°C, $10^{-1}s^{-1} + 10^{-2}s^{-1}$, (c) 350°C, $10^{-3}s^{-1}$, and (d) 350°C, $10^{-2}s^{-1} + 10^{-3}s^{-1}$. Percentage recrystallization, rex. grain size values in each case are labeled on the micrographs. The dark portions in the micrographs represent deformed regions.

It may be noted that at both temperatures (i.e. 425°C and 350°C), the use of two-step strain rate increased the total percentage of elongation. During the first step of the two-step strain rate, the formation of a large number of highly misoriented subgrains occurred. During the second step, such subgrains become the potential nuclei for the recrystallized grains. This process occurs throughout the microstructure as the deformation process progresses further. The resultant high angle boundaries slide and dominate the overall deformation process. In the present alloy containing both Zr and Sc as the dispersoid forming elements, the recrystallized grains are very stable against coarsening and the result is the high total percentage of elongation during the superplastic deformation. It is noteworthy that the use of two-step strain rate, therefore, not only accelerates the onset of recrystallization, but it also causes refinement of the recrystallized grains as well as an overall increase in the percentage recrystallization in the alloy.

4. Summary and Conclusions

1. High strength Al-Zn-Mg-Cu-Zr alloy 7010 containing 0.23 wt% Sc, where static recrystallization is extremely difficult, cannot and need not have "equiaxed recrystallized grains of size <10 μm" as the initial microstructure prior to superplastic deformation. The essentially unrecrystallized initial grain structure of the alloy, produced through a suitable thermo-mechanical process, undergoes continuous recrystallization during the superplastic deformation under appropriate combinations of temperature and strain rate. The percentage recrystallization and the average size of the recrystallized grains increase gradually with the percentage elongation. The final grain structure has an average recrystallized grain size of less than 10 μm under all superplastic deformation conditions studied in this work.
2. The utilization of two-step strain rate always has the effect of improving the total percentage elongation due to a combination of increased total percentage recrystallization and refinement of new grains. An elongation of as high as 916% was registered for the alloy when deformed at $425^{o}C$, $10^{-1}s^{-1}+ 10^{-2}s^{-1}$, and an elongation of 438% was recorded for the alloy when deformed at $350^{o}C$, $10^{-2}s^{-1} + 10^{-3}s^{-1}$.
3. The stability of the recrystallized grains against coarsening is the key toward the attainment of enhanced superplasticity in the alloy containing both Zr and Sc.

Acknowledgement

The authors wish to acknowledge the financial support of Defence Research and Development organization (DRDO), Government of India.

References

[1] A. K. Mukhopadhyay, A. Kumar and K. S. Prasad: Proc. ICAA11 (eds. J. Hirsch, B. Skrotski, G. Gottstein) DGM, Wiley-VCH GmbH & Co. KgaA, 1 (2008) 1782-1787.
[2] A. Kumar, A. K. Mukhopadhyay and K S. Prasad: Metall. Mater. Trans. 40A (2009) 278-281.
[3] A. Kumar, A. K. Mukhopadhyay and K. S. Prasad: Mater. Sci. Engg. A527 (2010) 854-857.
[4] T. G. Nieh, L. M. Hsuing, J. Wadsworth and R. Kaibyshev: Acta Mater. 46 (1998) 2789-2800
[5] Y. V. Milman, D. V. Lotsko and O. I. Sirko: Mater. Sci. Forum, 331-337 (2000) 1107-1112.
[6] J. Pilling and N. Ridley: Superplasticity in Crystalline Solids (London, The Institute of Metals, 1989).
[7] L. Qing, Y. Zinfeng and Y. Mei: Scripta Metall. Mater. 25 (1991) 109-114.
[8] M. H. Alvi, S. Cheong, H. Weiland and A. D. Rollet: Mater. Sci. Forum, 467-470 (2004) 357-362.
[9] S. Raveendra, S. Mishra, K. V. Hari Krishna, H. Weiland and I. Samajdar: Metall. Mater. Trans. 39A (2008) 2760-2771.